Automatic Fibroatheroma Identification from Intravascular Optical Coherence Tomography Images

Mengdi Xu[1], Jun Cheng[1], Jimmy Addison Lee[1], Guozhen Xu[1] and Damon Wing Kee Wong[1], Akira Taruya[2], Nicolas Foin[3], Philip Wong[3], and Atsushi Tanaka[2]

[1] Institute for Infocomm Research, Agency for Science, Technology and Research, Singapore (E-mail: xumd@i2r.a-star.edu.sg)
[2] Wakayama Medical Unviersity Japan
[3] National Heart Centre Singapore

Abstract. Vulnerable plaque identification is important in coronary heart disease diagnosis. Intravascular Optical Coherence Tomography (IVOCT) is an imaging modality which can characterize the appearance of vulnerable plaques. However, current used manual reading of the images is time consuming and subjective. Therefore, an automated and objective assessment of the plaque is necessary. This paper proposes a method for automatic identification of potential vulnerable plaque such as fibroatheroma in IVOCT images. In the proposed method, a graph search based method is applied to detect the region of interest (ROI) including the inner lumen border and outer border. Then various appearance features including the textures and the shape of ROI are extracted. A classifier is trained using support vector machine to detect the presence of fibroath eroma plaque in the IVOCT images. The proposed method is evaluated using a dataset of 200 images from 24 different pullbacks. Experimental results show that the proposed method achieves a mean accuracy of 90%, with sensitivity of 88% and specificity of 92%, in identifying fibroatheroma plaque in IVOCT images.

1 Introduction

Coronary artery disease is a common type of heart disease and cause of heart attacks. Identification of potential vulnerable plaque such as fibroatheroma, especially the thin-cap fibroatheroma (TCFA), is very important in coronary artery disease diagnosis. However, widely used imaging modality, such as intravascular ultrasound (IVUS), is unable to detect TCFA reliably, due to its limited resolution.Recently, intravascular optical coherence tomography (IVOCT) [1] [2] has become a promising intravascular diagnostic tool with a resolution of 15 μm, allowing a level of detail never achieved before. It is shown that IVOCT can assess fibroatheromas [2]. Currently, plaque characterization in IVOCT images is mainly conducted through manual reading by interventional cardiologist performing the IVOCT imaging. However, manual assessment is time-consuming

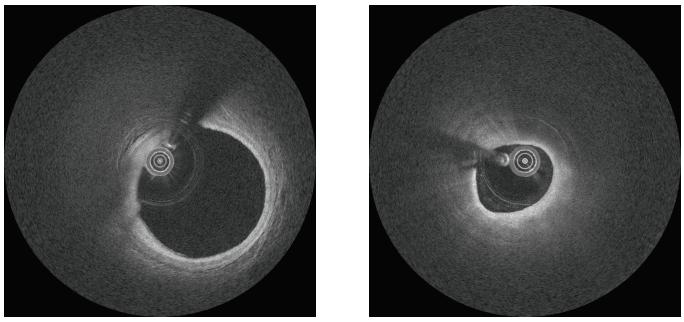

Fig. 1. (a) IVOCT image with normal vessel wall. (b)IVOCT image with fibroatheroma.

and subjective; therefore, an automated and objective assessment method is needed.

It has been shown that IVOCT is capable of detecting and quantifying specific lesion contents, owing to its high resolution [3]. In IVOCT, a fibroatheroma plaque appears as a region with poorly delineated borders and a cap. TCFA appears as a region with low backscattering and a thin fibrous cap ($< 65\mu m$). Fig. 1 shows sample IVOCT images with normal vessel wall and fibroatheroma. It can be seen that fibroatheroma has a low backscattering, signal-poor regions with diffuse border. In this paper, we focus on the identification of fibroatheroma from IVOCT images, which can be used for TCFA detection by further measuring the cap thickness.

Several automated or semi-automated IVOCT image analysis methods have been proposed for IVOCT image processing. The most recent one was proposed by Athanasious *et al.* [4]. They presented a fully automated methodology that was able to characterize the composition of the superficial plaque in FD-OCT images. The region between the lumen border and the expanded lumen border, which called tissue area, was detected and segmented. The pixels within tissue area were classified to four classes. Athanasious *et al.* [5] also proposed an automatic method for calcium detection. Some existing automatic works were based on backscattering and attenuation coefficient analysis. Xu *et al.* [6] studied the backscattering and attenuation coefficient in three tissue types including calcium, fibrous tissue and lipid tissue. Van Soest *et al.* [7] studied the attenuation coefficients of fibrous caps infiltrated by macrophages, lipid tissue, intimal thickening plaques and healthy segments. Ughi*et al.* [8] proposed an automated method for tissue characterization. They studied texture features and optical attenuation properties, and applied them to pixel-wise tissue characterization problem. An overall pixel-wise accuracy of 81.5% was achieved.

Different from the previous methods which attempt to detect the tissue types, we investigate the visual appearance of the IVOCT images and propose an automated method to identify the presence of potential vulnerable plaque such

as fibroatheroma by utilizing its appearance features. In our method, a graph search based algorithms is applied to detect the region of interest between the inner lumen border and outer border. Two classical texture features, the local binary pattern and the histogram orientated gradients are explored. In addition, the thickness of the region of interest is also used.

2 Method

This section introduces technical details of the proposed method. The proposed method includes following main steps: a) region of interest (ROI) detection, b) shape feature extraction, c) texture features extraction, and d) classification to detect the presence of fibroatheroma in IVOCT images.

2.1 Region of Interest Detection

The Region of interest (ROI) refers to the region between the inner lumen border and the outer border. In this paper, we use a graph search based method [9] to detect the inner lumen border and outer border.

Graph search based lumen segmentation In our method, we first convert the image into polar coordinate. Then each 2D IVOCT image is represented as a graph of nodes. The pixels (nodes) are connected through edges. A weight value, which represents the cost to pass through the edge, is assigned to each edge. The total cost for traveling from one node to another will be the sum of all weight values assigned to the edges that connecting the nodes. Usually, functions of distances between pixels or intensity values are used to assign weight values. After assigned the weight values, Dijkstra's algorithm [10] is used to determine the path of a graph between arbitrary endpoints with lowest sum weight. In our implementation, the weights are calculated based on intensity gradients:

$$w_{ab} = 2 - (g_a + g_b) + w_{min}, \tag{1}$$

where w_{ab} denotes the weight of the edge which connects node a and node b, g_a and g_b denote the vertical gradients of the image at node a and node b, respectively. w_{min} is a small positive number added to keep the system stable.

In the polar images, we search for a path starting from top-left of the image and ending at bottom right of the images. We apply Dijkstra's algorithm [10] to find the path with lowest cost to determine the inner lumen border. More details of the algorithms can be found in [9].

Outer border and Region of interest (ROI) In order to detect the ROI, we need to detect the outer border. Since the ROI is typically the brightest part of the image, we propose to detect the region via thresholding. However, a fixed threshold does not work well as the optical properties of different atherosclerotic

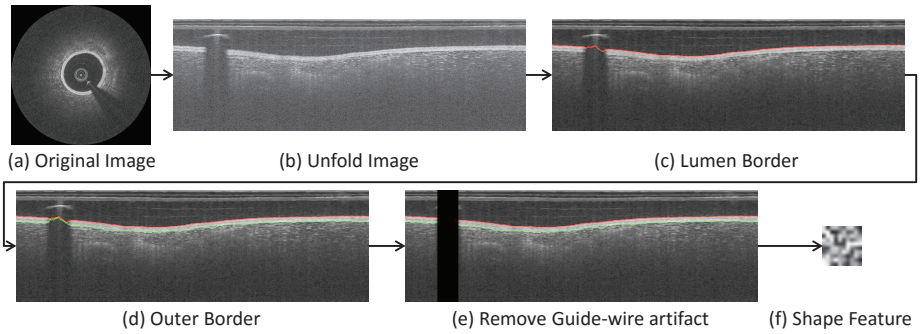

Fig. 2. Flowchart of shape feature extraction.(a) Original images. (b)Transform to Polar Coordinates. (c) Lumen segmentation. (d) Detect outer border. (e) Remove the guide-wire region. (f) Extract shape feature.

plaques varies and makes the different lumen have different brightness. In this paper, we first estimate the pixel intensity along the inner lumen border. For this purpose, we draw a line by moving the inner lumen border down vertically by a small value (15 pixels in this paper). Then the median pixel intensity between the inner lumen border and this line is computed and used as the threshold. A binary image is obtained after thresholding. Finally, we use the same graph search approach to get the outer border by detecting the bright to dark transition from the threshold image. We find this approach works well in most images even though a full quantitative evaluation is not yet provided in this paper. Fig. 2 illustrates the process to detect the ROI.

2.2 Shape Feature Extraction

The shape feature describes the shape properties between the inner lumen border and the outer border. To find the shape features, we first compute the distance vector $D = [D_1, D_2, ...D_N]$, between two boundaries at each column in the polar image, where N is the number of columns in the polar image. Guide-wire artifact is detected using our earlier sliding window based method [11]. Distance values within guide-wire artifact region$P$, $P = (p_1, p_2, ...p_a)$, are removed to get the final distance vector D', $D' = [D_1, D_2, ..., D_{p_1-1}, D_{P_a+1}, ..., D_N]$. Here a is the length of guide-wire artifact. For fibroatheroma, the shortest distance between inner lumen border and outer border is always very small while the longest distance will not be too large. Thus we sort the distance vector in descending order, and compute the mean value for the top ten and bottom ten elements. The 2-D vector $[mean(D'_{top10}), mean(D'_{bottom10})]'$ is the final shape feature.

2.3 Texture Feature Extraction

Besides shape feature, we also explored the classic texture features, local binary pattern (LBP) bag-of-words (BOW) and histogram of oriented gradient (HoG)

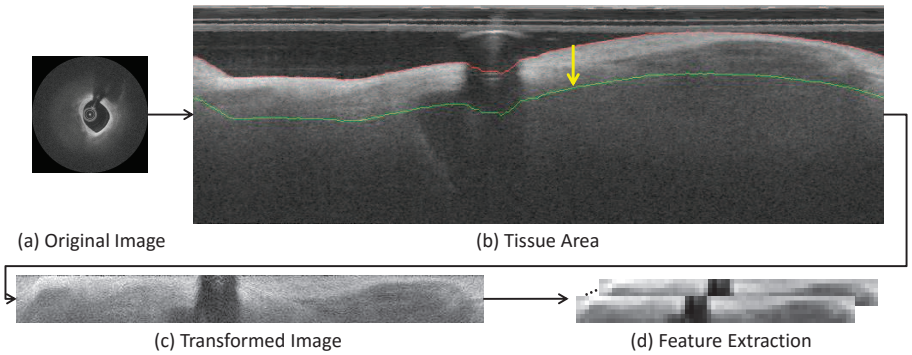

Fig. 3. Texture feature extraction scheme. (a) Original image. (b) Transform the original image to Polar Coordinates, and detect texture region. (c) Transform the texture region to rectangle. (d) Extract texture features.

BOW. Fig. 3 illustrates texture features extraction process. We first transform the original image to polar coordinates, then apply graph based method to get lumen border. After that, we extend the lumen border down to 48 pixels vertically, and get the texture region, which including the majority texture information. We transform the texture region to rectangle image, and finally extract texture features on the transformed image.

Two texture features, LBP BOW and HOG BOW are extracted to describe the texture. To construct BOW codebooks, we compute LBP and HOG features for training images, and use K-means clustering method to get the codebook centres. We set $K = 32$ for LBP and HOG, empirically.

2.4 Classification

After feature extraction, we apply Support Vector Machine (SVM) [12] to determine whether the input IVOCT image contains fibroatheroma. In this experiment, LIBSVM package [13] is employed for classification.

3 Experimental Results

3.1 Dataset

The data used in this paper were collected using TERUMO optical frequency domain imaging (OFDI) at Wakayama Medical University. A total of 24 pullbacks from different subjects are used, among which, 12 pullbacks are used for training and the rest of 12 pullbacks are used for testing. The OCT images in our dataset are resized to 512×512.

Since continues neighboring scans from the same pullback are often similar, we use images from different locations with at least 5 scans apart from each other

from each pullback. In order to train a classifier to detect fibroatheroma, a total of 50 images with fibroatheroma plaque and 50 images without fibroatheroma plaque are selected from the 12 training pullbacks for training. Then, 50 images with fibroatheroma plaque and 50 images without fibroatheroma plaque are also selected from the 12 testing pullbacks for testing. As we obtain training and testing images from different subjects, we do not need to worry about the overfitting due to potential contents similarity of images from same subject.

3.2 Results

In the training process, a standard two-fold cross validation is utilized to determine the SVM parameter. In order to justify the effectiveness of the individual features, we conduct the experiments when we use only the individual features as well as a combination of these features. Then sensitivity P_+, i.e., the proportion of positive samples which are correctly identified, and specificity P_-, i.e., the proportion of negative samples which are correctly identified, as well as their average $P = (P_+ + P_-)/2$ are computed to evaluate the performance. Table 1 shows the classification results.

Table 1. Classification Accuracy.

	Shape	*LBP*	*HOG*	*Shape+LBP+HOG*
Sensitivity P_+	0.68	0.84	0.70	0.88
Specificity P_-	0.50	0.86	0.86	0.92
Accuracy P	0.59	0.85	0.78	0.90

As shown in Table 1, for single features, HOG and LBP outperforms the shape features, which indicating that texture is crucial in fibroatheroma identification. By integrating the shape feature with LBP and HOG features, the classification accuracy increases to 90%. Which means that the shape feature is also a useful component in fibroatheroma identification.

Fig. 4 shows some sample results of lumen border and outer border detection. Here (b) shows IVOCT image with fibroathercoma, (a) (c) (d) shows IVOCT images not with fibroatheroma. Red line shows the inner lumen border, green line shows outer border, and yellow region shows guide-wire artifact. As illustrated in the figure, the area between lumen border and outer border contains most significant information and features, and the outer border demonstrates the shape varies for different lesions. Thus it is reasonable to use the distance between lumen border and outer border to classify the IVOCT images.

4 Conclusions

In this work, we propose an automated method to detect the presence of fibroatheroma from IVOCT images. By integrating the HOG, LBP and shape

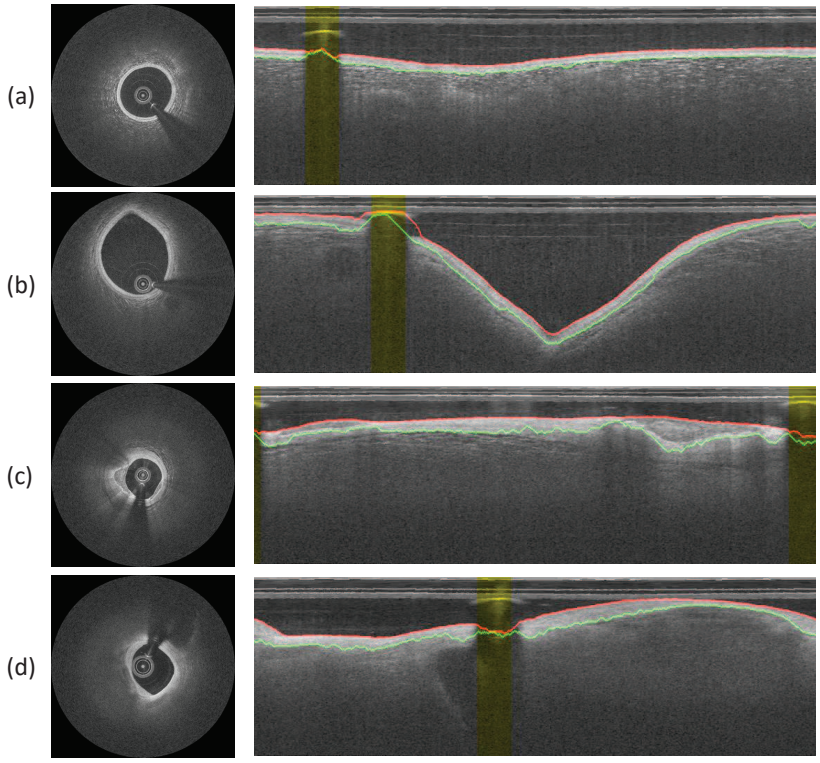

Fig. 4. Results of lumen and outer border detection.

features, the proposed method is able to achieve an average accuracy of 90%. This work could be used as a preprocess in plaque characterization to reduce the burden of cardiologists.

Acknowledgment

This project is supported in partial by Agency of Science, Technology and Research grant 152-148-0026.

References

1. Prati, F., Regar, E., Mintz, G.S., Arbustini, E., Di M., C., Jang, I.K., Akasaka, T., Costa, M., Guagliumi, G., Grube, E., et al.: Expert review document on methodology, terminology, and clinical applications of optical coherence tomography: physical principles, methodology of image acquisition, and clinical application for assessment of coronary arteries and atherosclerosis. European heart journal **31** (2010) 401–415

2. Prati, F., Guagliumi, G., Mintz, G.S., Costa, M., Regar, E., Akasaka, T., Barlis, P., Tearney, G.J., Jang, I.K., Arbustini, E., et al.: Expert review document part 2: methodology, terminology and clinical applications of optical coherence tomography for the assessment of interventional procedures. European heart journal **33** (2012) 2513–2520
3. Tearney, G.J., Regar, E., Akasaka, T., Adriaenssens, T., Barlis, P., Bezerra, H.G., Bouma, B., Bruining, N., Cho, J.m., Chowdhary, S., et al.: Consensus standards for acquisition, measurement, and reporting of intravascular optical coherence tomography studies: a report from the international working group for intravascular optical coherence tomography standardization and validation. Journal of the American College of Cardiology **59** (2012) 1058–1072
4. Athanasiou, L.S., Bourantas, C.V., Rigas, G., Sakellarios, A.I., Exarchos, T.P., Siogkas, P.K., Ricciardi, A., Naka, K.K., Papafaklis, M.I., Michalis, L.K., et al.: Methodology for fully automated segmentation and plaque characterization in intracoronary optical coherence tomography images. Journal of biomedical optics **19** (2014) 026009–026009
5. Athanasiou, L.S., Bourantas, C.V., Rigas, G.A., Exarchos, T.P., Sakellarios, A.I., Siogkas, P.K., Papafaklis, M.I., Naka, K.K., Michalis, L.K., Prati, F., et al.: Fully automated calcium detection using optical coherence tomography. In: Engineering in Medicine and Biology Society (EMBC), IEEE (2013) 1430–1433
6. Xu, C., Schmitt, J.M., Carlier, S.G., Virmani, R.: Characterization of atherosclerosis plaques by measuring both backscattering and attenuation coefficients in optical coherence tomography. Journal of biomedical optics **13** (2008) 034003–034003
7. Van Soest, G., Goderie, T., Regar, E., Koljenović, S., van Leenders, G.L., Gonzalo, N., van Noorden, S., Okamura, T., Bouma, B.E., Tearney, G.J., et al.: Atherosclerotic tissue characterization in vivo by optical coherence tomography attenuation imaging. Journal of biomedical optics **15** (2010) 011105–011105
8. Ughi, G.J., Adriaenssens, T., Sinnaeve, P., Desmet, W., Dhooge, J.: Automated tissue characterization of in vivo atherosclerotic plaques by intravascular optical coherence tomography images. Biomedical optics express **4** (2013) 1014–1030
9. Xu, M., Cheng, J., Wong, D.W.K., Liu, J., Taruya, A., Tanaka, A.: Graph based lumen segmentation in optical coherence tomography images. In: 2015 10th International Conference on Information, Communications and Signal Processing (ICICS), IEEE (2015) 1–5
10. Dijkstra, E.W.: A note on two problems in connexion with graphs. Numerische mathematik **1** (1959) 269–271
11. Xu, M., Cheng, J., Wong, D.W.K., Taruya, A., Tanaka, A., Liu, J.: Automatic atherosclerotic heart disease detection in intracoronary optical coherence tomography images. In: Engineering in Medicine and Biology Society (EMBC), IEEE (2014) 174–177
12. Cortes, C., Vapnik, V.: Support-vector networks. Machine learning **20** (1995) 273–297
13. Chang, C.C., Lin, C.J.: LIBSVM: A library for support vector machines. ACM Transactions on Intelligent Systems and Technology **2** (2011) 27:1–27:27 Software available at http://www.csie.ntu.edu.tw/ cjlin/libsvm.